Fabrication and replication of re-entrant structures by nanoimprint lithography methods

Nikolaos Kehagias, Achille Francone, Markus Guttmann, Frank Winkler, Ariadna Fernández, and Clivia M. Sotomayor Torres

---

ARTICLES YOU MAY BE INTERESTED IN

In-line metrology for roll-to-roll UV assisted nanoimprint lithography using diffractometry
APL Materials **6**, 058502 (2018); https://doi.org/10.1063/1.5011740

Nanoimprint lithography: An old story in modern times? A review
Journal of Vacuum Science & Technology B: Microelectronics and Nanometer Structures Processing, Measurement, and Phenomena **26**, 458 (2008); https://doi.org/10.1116/1.2890972

Wafer-scale fabrication of CMOS-compatible, high aspect ratio encapsulated nanochannels
Journal of Vacuum Science & Technology B **36**, 051801 (2018); https://doi.org/10.1116/1.5034463

Investigating the interplay of lateral and height dimensions influencing neuronal processes on nanogrooves
Journal of Vacuum Science & Technology B **36**, 06J801 (2018); https://doi.org/10.1116/1.5048069

Nanoimprint lithography
Journal of Vacuum Science & Technology B: Microelectronics and Nanometer Structures Processing, Measurement, and Phenomena **14**, 4129 (1996); https://doi.org/10.1116/1.588605

Moth-eye antireflection nanostructure on glass for CubeSats
Journal of Vacuum Science & Technology B **36**, 06JG01 (2018); https://doi.org/10.1116/1.5050986

Fabrication and replication of re-entrant structures by nanoimprint lithography methods

Nikolaos Kehagias,[1,a)] Achille Francone,[1] Markus Guttmann,[2] Frank Winkler,[2] Ariadna Fernández,[1,3] and Clivia M. Sotomayor Torres[1,4]

[1]Catalan Institute of Nanoscience and Nanotechnology (ICN2), CSIC and BIST, Campus UAB, Bellaterra, 08193 Barcelona, Spain
[2]Karlsruhe Institute of Technology (KIT), Institute of Microstructure Technology, D-76344 Eggenstein Leopoldshafen, Germany
[3]INL—International Iberian Nanotechnology Laboratory, Avenida Mestre José Veiga, 4715-330 Braga, Portugal
[4]ICREA (Institució Catalana de Recerca i Estudis Avançats), 08010 Barcelona, Spain

In this work, the authors present and demonstrate a simple method to fabricate and mass replicate re-entrant structures. The method consists of the direct imprinting of polymer mushroomlike microstructures produced by a combination of photolithography and nickel up-plating process. In particular, they have studied the conditions to generate highly robust mushroomlike topographies and their topographical impact on the replication process. They discuss all the imprinting conditions suitable to replicate such topographies using both ultraviolet light assisted nanoimprint lithography (UV-NIL) and thermal NIL methods in two polymer films, poly(methyl methacrylate) and polypropylene, and a hybrid (organic–inorganic) UV light curable photoresist, namely, Ormocomp. Re-entrant topographies have been widely studied for liquid/oil repelling and dry adhesive properties, whereas in their experiments, they have proved evidence for their amphiphobic potential. © 2018 Author(s). All article content, except where otherwise noted, is licensed under a Creative Commons Attribution (CC BY) license (http://creativecommons.org/licenses/by/4.0/). https://doi.org/10.1116/1.5048241

I. INTRODUCTION

Most of the common contaminants and pollutants are based on organic materials, which adhere on the surfaces and do not repel easily. Numerous studies have demonstrated superhydrophobic surfaces with water contact angles (WCAs) greater than 150° and low WCA hysteresis.[1] Engineered surfaces that show low affinity toward most of the low surface tension liquids (exp. oils) are not achievable unless low surface energy and re-entrant are present. Studies have shown that a liquid faces difficulty to enter a pattern with an overhanging structure due to the capillary force acting at the solid/liquid interface. As a result, the liquid cannot touch the bottom of the pattern and a layer with trapped air is formed on the surface.[2,3]

Figure 1 illustrates two types of topographies, a concave [Fig. 1(a)] and a convex structure [Fig. 1(b)], whereas in both cases, the liquid contacting the structure in the Cassie–Baxter state locally displays a contact angle (CA) equal to Young's contact angle. For the concave case, the Cassie–Baxter state is possible only if Young's contact angle is greater than 90°, while for the convex topography, the Cassie–Baxter state can be obtained also for liquids having a Young contact angle lower than 90°.

Recent approaches have employed chemically modified materials such as glass and silicon oxides or polymers to create re-entrant surfaces mainly for oil-repellent applications.[4,5] However, the efficient fabrication and mass replication of micro- and nanostructures with re-entrant or overhang structures still remains a bottleneck. All the reported fabrication methods involve complicated, high-cost, and nonflexible approaches lacking high-throughput manufacturing projections.

Nanoimprint lithography[6] (NIL) is an alternative[7] toward the conventional fabrication methods due to its high resolution, low cost of ownership, and high-throughput capability to process hybrid materials and substrates. Moreover, the topographical features present on a mold or stamp can be replicated into a thin layer of bulk resist materials via different mechanisms, such as thermal nanoimprint[8] and/or ultraviolet light assisted nanoimprint (UV-NIL)[9] or reverse nanoimprint lithography.[10–12]

In this paper, we report a novel fabrication method to realize re-entrant structures by means of UV-NIL and thermal NIL. Combining photolithography and electrodeposition process, we produce nickel mushroomlike structures. To mass replicate our topographies, we used a negative soft particle desorption mass spectrometry (PDMS) stamp to imprint in a hybrid UV curable resist material or in bulk polymer films.

Our produced re-entrant topographies were appropriate to generate a superhydrophobic state of water due to the fact that the overhang structures promoted air trapping creating a composite interface. However, due to the low surface tension of oils, the surfaces were limited to an oleophobic state to various oils. After the treatment of the produced overhanging structures with a low surface energy coating, enhanced repellence was observed over a wide range of low surface tension liquids, as well as small sliding angles, indicating the Cassie–Baxter state.

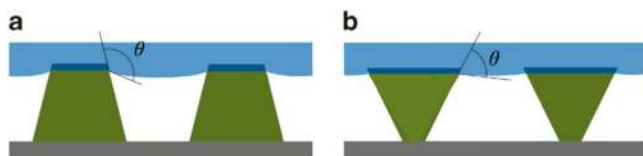a)Electronic mail: nikos.kehagias@icn2.cat

FIG. 1. (a) Schematic of a concave texture showing a water liquid droplet in the Cassie–Baxter state. (b) A schematic of a convex re-entrant structure showing a lower surface tension liquid with $\theta < 90°$ in the Cassie–Baxter state.

II. EXPERIMENT

A. Fabrication steps of re-entrant nickel structures

Our nickel re-entrant structures were realized on a silicon wafer by means of photolithography and electroplating techniques. Our silicon wafers were metal coated with a 50 nm Au layer on top of a 5 nm Cr layer [Fig. 2(a)] by electron beam evaporation. The Cr layer provided the appropriate adhesion for the Au layer which acted as our conductive seed layer for the nickel up-plating process. Depending on the targeted feature sizes, we spin coated on the silicon/Cr/ Au wafer a photoresist (AZ nLoF2035 or AZ 5214E) and subsequently exposed it to UV light through a positive quartz photolithography mask. The layout and dimensions of the targeted structures were represented on the mask which contained a square array of circles of 2, 4, and 10 μm diameter having a pitch of 6, 11, and 25 μm, respectively. In all cases, the aspect ratio of our structures was targeted to be 1:1. A development step followed the photolithography in order to open the necessary window holes in the resist [Fig. 2(b)]. It is important that there is no residual polymer left after the photolithography and development step as any residuals will cause poor adhesion of the grown nickel structures toward the Au/Cr coated silicon substrate.

Following the photolithography step, our samples were placed in a standard electroplating bath containing a mix of nickel sulfamate [Ni(SO$_3$N$_2$)$_2$] ($\sim$80 g/l Ni), boric acid (H$_3$BO$_3$) ($\sim$40 g/l), and a fluoride surfactant ($\sim$180 mg/l). The bath solution was kept at a constant temperature of

52 °C keeping the pH level between 3.4 and 3.6, while the current density was between 0.1 and 0.5 A/dm^2. By varying the electroplating time, we could control the nickel height in an additive manner filling the holes and eventually overgrowing the nickel features from the patterned polymer holes. The uniform overgrown nickel formed the desired mushroomlike shape of our re-entrant structures [Fig. 2(c)]. Consequently, the photoresist layer was stripped using acetone and oxygen plasma [Fig. 2(d)] to fully leave behind complete metallic structures (Fig. 3).

B. Fabrication of re-entrant polymer structures by UV-NIL

The produced nickel structures were treated with a fluorinated antiadhesion layer to alter its surface energy for easy mold release. Subsequently, a soft PDMS (Sylgard 184, Dow Corning, USA) replica was fabricated [Figs. 2(e) and 2(f)] by casting the PDMS prepolymer against the relief structure of the nickel template. A 10:1 ratio (precursor:curing agent) was mixed and cured for 12 h at 60 °C. The final thickness of the PDMS mold was between 2 and 3 mm. This factor enhances the mechanics of the demolding process and enhances the easiness of replication. The UV curable resist used throughout our experiments was Ormocomp purchased from *microresist technology GmbH*. Ormocomp is a hybrid UV curable resist qualified to be cured under atmospheric conditions. Our resist was spin coated at 3000 rpm for 1 min on a silicon wafer while the PDMS mold was placed on the resist surface in a liquid phase [Fig. 2(g)]. A "soft" air pressure of 3 bar was applied for 30 s followed by a UV light flood exposure for 5 s [Fig. 2(h)].

Although great efforts have been made on enhancing the opportunities and applications of NIL, it still remains to demonstrate that this technique is suitable to replicate overhanging structures with a high overhanging degree.[13,14]

When the density of our mushroomlike structures overpasses a critical spacing width, the demolding of these topographies
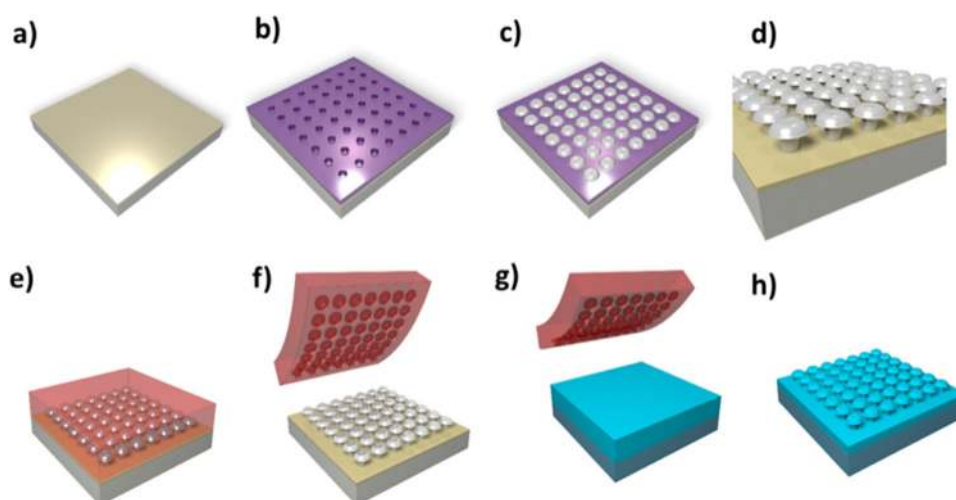

FIG. 2. [(a)–(h)] Schematic of the fabrication process followed to develop the polymeric mushroomlike structures. The template was fabricated on nickel by electrodeposition [(a)–(d)]. A soft stamp was produced with the negative pattern [(e) and (f)]. This soft stamp was used to produce mushroomlike structures by direct UV-NIL [(g)–(h)].
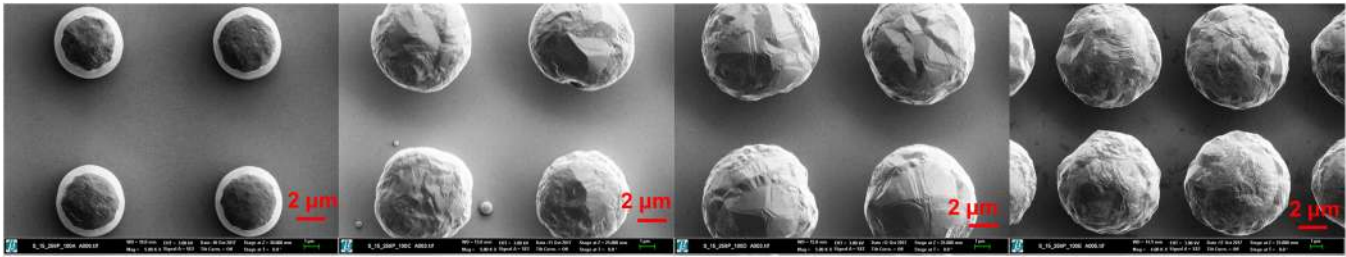
FIG. 3. Top view SEM images illustrating the increase of the filling factor as the nickel electroplating process increases in time. $4\,\mu m$ base diameter structures (from left to right) additively grown for 2, 4, 5, and 6.5 h decreasing the interspace distance of the mushroom caps.

is not possible and the structures fragment. Our PDMS mold has limited strength to separate from the imprinted structures and is therefore amended. Scanning electron microscopy (SEM) inspection of this factor can be seen in Fig. 4(b), where PDMS has been trapped within the underlying areas of the mushroom caps during the demolded step. This factor is attributed to the limited spacing between the mushroom caps and the shrinkage limit of PDMS. When the cap interspace increases, the underlying PDMS material (mold) finds the necessary space to release itself and provide a good replication. Moreover, the mechanical durability of our embossed Ormocomp material plays an important role in the overall ability to demold overhanging structures. A significant aspect for the overall process is the thick ($>20\,\mu m$) residual layer of the Ormocomp material (in the UV-NIL approach). Experimental investigations show that one having thin residual layer delamination of the Ormocomp material and the silicon substrate appears. Figure 4 (left) presents the fragment of the soft PDMS mold and its residue on the micropatterned substrate (Si/Ormocomp) when the interspacing distance has reached its critical point. The image of Fig. 4 (right) shows our working PDMS mold containing the negative re-entrant features.

C. Fabrication of re-entrant polymer structures by thermal NIL

Just like in the case of UV-NIL, we have effectively used the PDMS mold as our working mold to thermally replicate

the re-entrant structures in bulk polymer films. In particular, we have used two commercial polymers poly(methyl methacrylate) (PMMA; thickness: $125\,\mu m$) and polypropylene (PP; thickness: $100\,\mu m$) to replicate the mushroomlike topographies. Despite the perception that structures with overhanging features cannot be replicated by molding techniques, we prove that NIL is a flexible and versatile technique to replicate topographies with three-dimensional features. Table I summarizes the embossing parameters used throughout our experimental validations. All thermal imprinting experiments were carried out on a desktop CNI tool from NILTechnology ApS.

Three types of re-entrant topographies were fabricated with the process described in Fig. 5. Individual 4-in. wafers containing 2, 4, and $10\,\mu m$ mushroom "trunk" diameters were produced with overhanging protrusions (mushroom caps) of 4, 5, and $18\,\mu m$, respectively.

D. Characterization of the re-entrant structures

To improve the water repelling behavior of the produced Ormocomp re-entrant surfaces, a fluorosilane treatment was performed. The combination of the chemical treatment and the overhanging structures enables the formation of a favorable liquid–air interface for lower surface tension liquids, such as oils, that exhibit contact angles less than 90° on the corresponding flat surface.

The static CA of different liquids was measured by a contact angle analyser (Kruss EasyDrop Standard). The CA
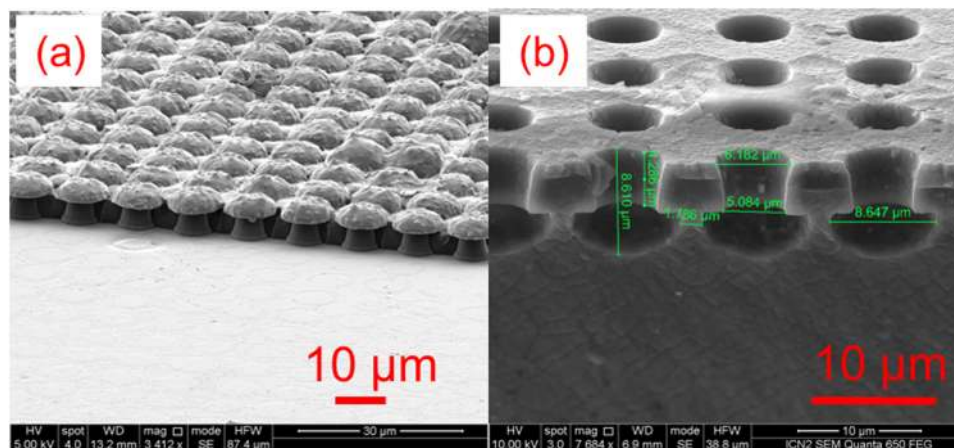

FIG. 4. Tilted view (70°) SEM image of (a) residual of PMDS mold remaining in the underlying areas of the re-entrant structures and (b) cross-section (90°) SEM image of our PMDS mold.

TABLE I. Thermal NIL processing parameters for two different polymer films.

	Imprint temperature (°C)	Pressure (bar)	Time (min)	Demolding temperature (°C)
PMMA	230	3	5	40
PP	200	3	5	40

was measured by gently placing a water droplet of $5\,\mu$l on the surface. The sliding angle was calculated by introducing a tilting stage and calculated as the angle at which the droplet starts to roll-off. The hysteresis was measured as the difference between the advanced and the receding contact angle, which were measured by increasing and decreasing the volume of the droplet, respectively. The presented values were averaged over at least five points on each sample. SEM images were taken using an FEI Quanta 650 FEG at an acceleration voltage of 5 kV and a working distance of 10 mm.

III. RESULTS AND DISCUSSION

A. Morphology control

Mushroomlike structures were successfully produced by a one-step electrodeposition process. Apart from the great advantage of having a one-step process, this method is highly controllable, allowing one to produce large area mushroomlike structures with different degrees of overhanging values.

Figure 6 depicts different samples with different sizes of the mushroom "caps." From SEM inspection, one can observe the alternating densities corresponding to surface morphologies of the samples produced at different electroplated times. Figures 6(a) and 6(d) correspond to a "low" degree of overhanging, corresponding to an intercap distance between 4.5 and 4.7 μm. Figures 6(b) and 6(e) correspond to a "medium" degree of overhanging, with the distance between the mushroom caps being between 2.5 and 2.7 μm, while Figs. 6(c) and 6(f) correspond to a "high" degree interspace distance of 1.2–1.7 μm.

The control of the morphology is a key issue since the surface needs to exhibit a good degree of overhanging to avoid water penetration and at the same time it needs to have a low solid–liquid contact fraction. For this reason, in this work, different mushroomlike structures were fabricated in order to find the optimum overhanging degree needed to obtain good water repellence.

Figure 6 shows top view and tilted view (70°) SEM images of Ormocomp and PP imprinted features, respectively, for three different filling factors, which correspond to three different degrees of overhanging features.

B. Surface wetting characterization

Surface wetting characterization was performed on the UV-NIL fabricated surfaces. The low surface energy, combined with the rough surface texture, led to a
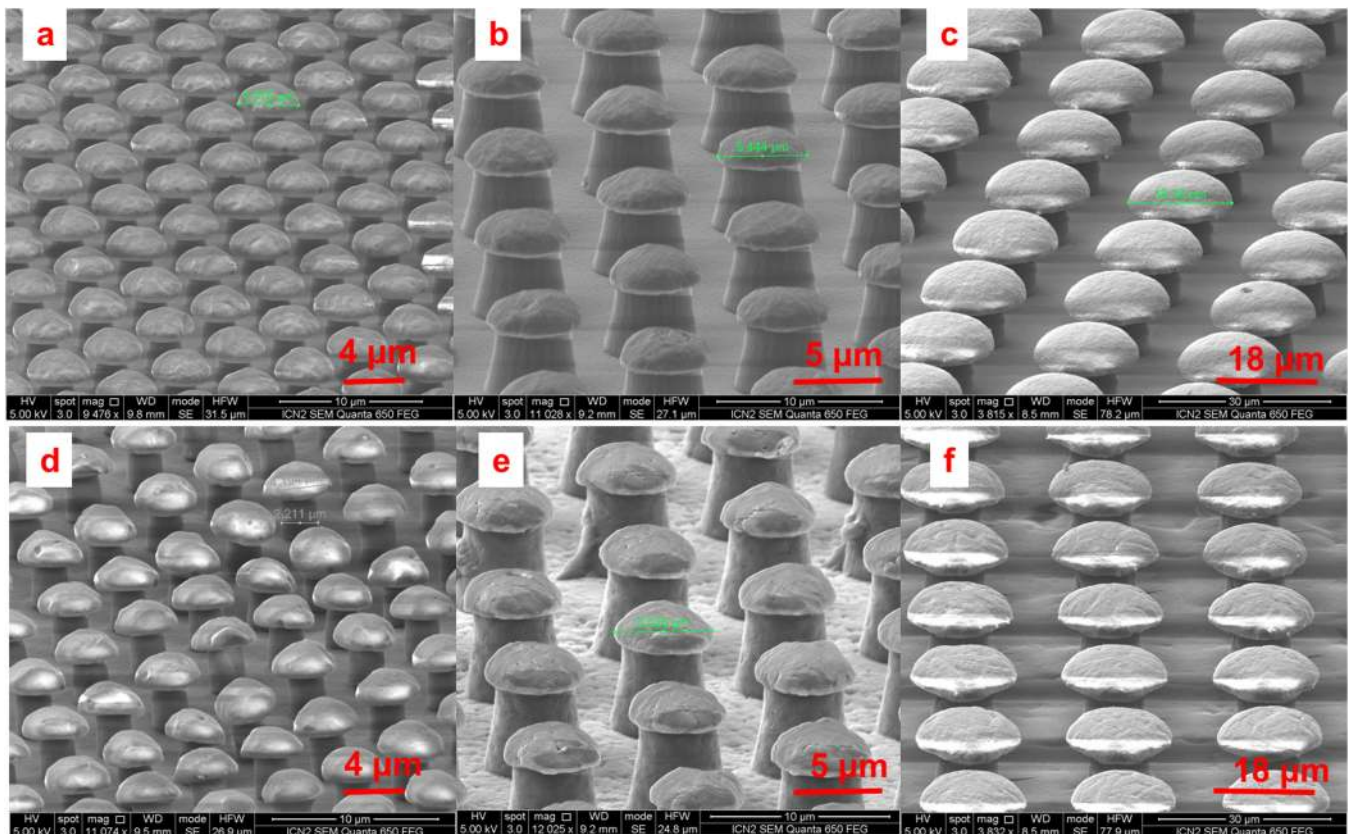

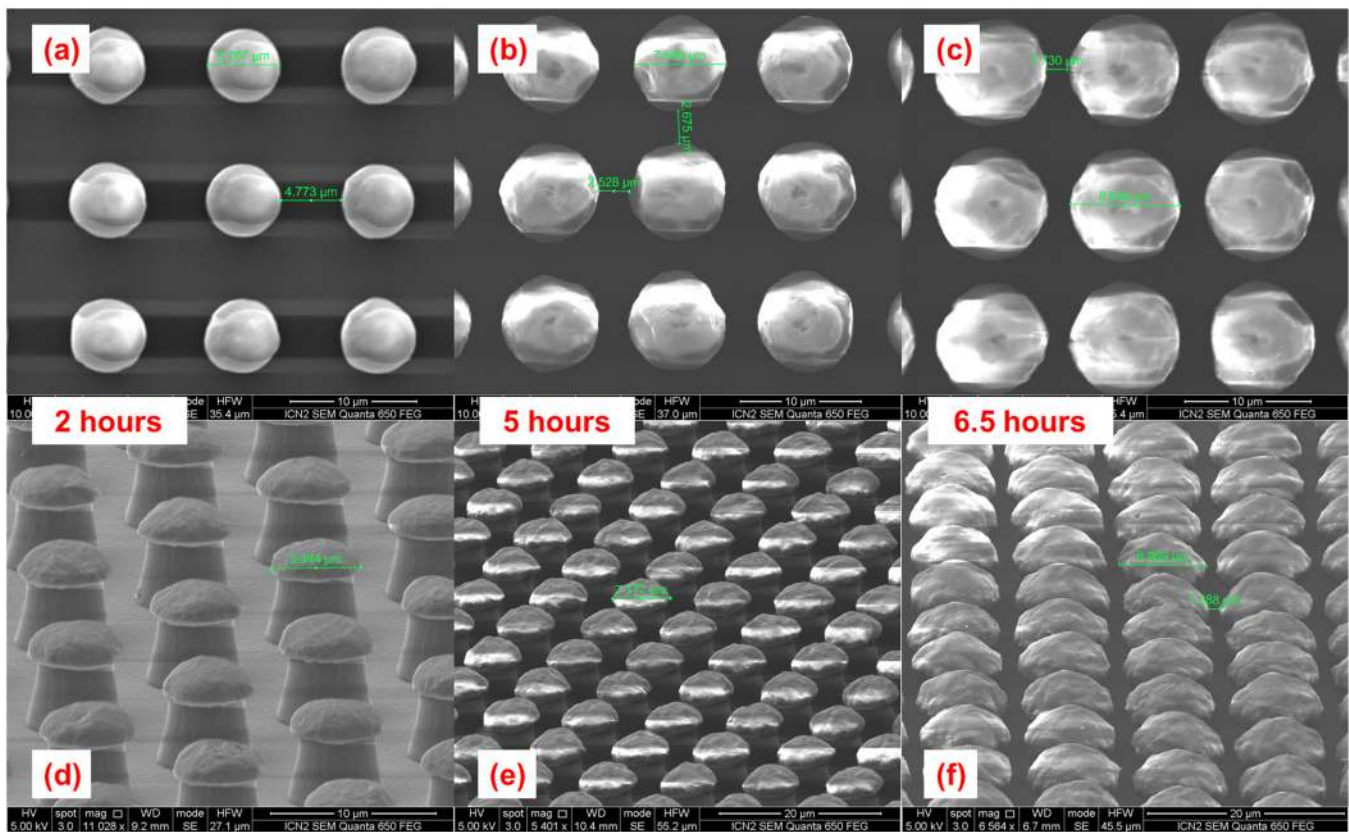FIG. 5. Tilted view SEM images of 2, 4, and 10 μm features imprinted in bulk PMMA [(a)–(c)] and PP [(d)–(f)] films.

FIG. 6. SEM images of representative imprints showing re-entrant structures of $4\,\mu m$ base diameter with three different degrees of densities. (a)–(c) illustrate imprinted features in an Ormocomp UV resist material, while (d)–(f) illustrate imprints in the bulk PP material.

superhydrophobic and oleophobic surface. Table II shows the static and dynamic WCA measurements and their standard deviation on the different fabricated mushroomlike structures. Treated flat Ormocomp surfaces were found to be hydrophobic with WCAs of 112°. Structured Ormocomp with a fluorine treatment resulted in having superhydrophobic behavior with WCAs as high as 155° and sliding angles as low as 8°. From the fabricated samples, the best superhydrophobic behavior was obtained for the mushroomlike structures with medium overhanging degree values. This can be explained due to the solid–liquid contact fraction existing for different structures.

A commercial droplet shape analysis instrument from Kruss was used to measure the wetting behavior of our prepared superhydrophobic surfaces. A water droplet (smaller than the capillary length) was gently placed on the surface using a needle and its contact angle value is measured using the sessile droplet method.[15] A camera and computer-controlled commercial software were used to measure the static CA after the needle was removed. To measure the hysteresis angle, a syringe was used to add and subtract water to and from the droplet which is resting on our structured surfaces. When a small amount of water is removed from the droplet, the droplet will recede with a constant contact angle, which is the receding contact angle (θ_R). When the water is added to the droplet, the droplet grows while the contact angle is maintained at the advancing contact angle (θ_A).

For the case of a low overhanging degree (low density structures), although the solid–liquid contact fraction is low, the great distance between adjacent mushrooms produces a partial penetration of the droplet meniscus, leading to a decrease in the contact angle value. For the case of high overhanging degree (high density structures), the solid–liquid contact fraction becomes higher due to the small distance between adjacent re-entrant structures.

Analogous WCA measurements have been commenced for the patterned PMMA and PP films containing re-entrant topographies with varying diameters and filling factors. Our investigations demonstrate that independent from the feature sizes (2, 4, and $10\,\mu m$ base diameter) and the material's intrinsic surface energy values, the WCA values fall within a similar range of 131°–136° having a high

TABLE II. Experimental WCAs measurements for the Ormocomp mushroomlike structures with different overhanging degrees.

Surface structure	Contact angles (°)		
	Static	Sliding	Hysteresis
Flat surface	112 ± 3	35 ± 3	40 ± 6
Low overhanging degree	148 ± 3	11 ± 4	10 ± 4
Medium overhanging degree	155 ± 1	8 ± 2	6 ± 3
High overhanging degree	147 ± 3	15 ± 3	12 ± 5

hysteresis angle (>20°). This factor reveals that although our patterned surfaces feature and increase in the WCA, in comparison to the flat unpatterned PMMA and PP bulk surfaces, the water droplets are stabilized exhibiting a pinning effect thus being in the Wenzel state. Although all produced re-entrant surfaces possess a hydrophobic state, superhydrophobicity with low hysteresis angles is achieved only when our imprinted material features a low surface energy value.

IV. SUMMARY AND CONCLUSIONS

In summary, we have developed a new fabrication approach to produce re-entrant structures utilizing a combination of top down (imprint lithography) and bottom up (electroforming) processes. Our master stamp containing mushroomlike structures was realized by combining nickel electrodeposition and photolithography. We have demonstrated that NIL is an alternative replication technique suitable to reproduce re-entrant structures when using a flexible PDMS stamp. The produced mushroomlike structures exhibited high static WCA values (155°) with low hysteresis angles (6°). Due to the nature of the re-entrant topographies, these surfaces open the path toward generating dynamic and reversible surfaces with engineered amphiphobic properties.

[1]B. N. Sahoo and B. Kandasubramanian, RSC Adv. **4**, 22053 (2014).
[2]P. S. Brown and B. Bhushan, APL Mater. **4**, 015703 (2016).
[3]M. Nosonovsky and B. Bhushan, Philos. Trans. R. Soc. London Ser. A **374**, 2073 (2016).
[4]T. P. N. Nguyen, R. Boukherroub, V. Thomy, and Y. Coffinier, J. Colloid Interface Sci. **416**, 280 (2014).
[5]H. J. Choi, S. Choo, J. H. Shin, K. I. Kim, and H. Lee, J. Phys. Chem. C **117**, 24354 (2013).
[6]S. Y. Chou, J. Vac. Sci. Technol. B **15**, 2897 (1997).
[7]H. Schift, J. Vac. Sci. Technol. B **26**, 458 (2008).
[8]S. Y. Chou, P. R. Krauss, and P. J. Renstrom, Science **272**, 85 (1996).
[9]J. Haisma, M. Verheijen, K. Van den Heuvel, and J. Van den Berg, J. Vac. Sci. Technol. B **14**, 4124 (1996).
[10]X. D. Huang, L. R. Bao, X. Cheng, L. J. Guo, S. W. Pang, and A. F. Yee, J. Vac. Sci. Technol. B **20**, 2872 (2002).
[11]N. Kehagias *et al.*, Nanotechnology **18**, 175303 (2007).
[12]A. Fernández, J. Medina, C. Benkel, M. Guttmann, B. Bilenberg, L. H. Thamdrup, T. Nielsen, C. M. Sotomayor Torres, and N. Kehagias, Microelectron. Eng. **141**, 56 (2015).
[13]S. Möllenbeck, N. Bogdanski, H. C. Scheer, J. Zajadacz, and K. Zimmer, Microelectron. Eng. **86**, 608 (2009).
[14]H. Schift, Appl. Phys. A **121**, 415 (2015).
[15]M. Strobel and C. S. Lyons, Plasma Process. Polym. **8**, 8 (2011).